Int. J. Electrochem. Sci., 9 **(2014)** 5993 - 6005

International Journal of
ELECTROCHEMICAL
SCIENCE
www.electrochemsci.org

Determination of Corrosion Inhibition Efficiency Using HPHT Autoclave by *Gingko biloba* on Carbon Steels in 3.5% NaCl solution Saturated with CO_2

Ambrish Singh[1,2], *Yuanhua Lin*[1,*], *Eno E. Ebenso*[3], *Wanying Liu*[1], *Bo Huang*[4]

[1] State Key Laboratory of Oil and Gas Reservoir Geology and Exploitation, Southwest Petroleum University, Chengdu- 610500, Sichuan, China.
[2] Department of Chemistry, School of Civil Engineering, LFTS, Lovely Professional University, Phagwara-144402, Punjab, India.
[3] Department of Chemistry, School of Mathematical & Physical Sciences, North-West University(Mafikeng Campus), Private Bag X2046, Mmabatho 2735, South Africa.
[4] CNPC Key Lab for Tubular Goods Engineering (Southwest Petroleum University), Chengdu, Sichuan 610500, China
[*]E-mail: yhlin28@163.com; vishisingh4uall@gmail.com

Received: 9 June 2014 / *Accepted:* 29 July 2014 / *Published:* 25 August 2014

Leaves extract of *Gingko biloba* (GBE) was characterized using mass spectrometry (MS) and Fourier transform infrared spectroscopy (FTIR) methods. The influence of GBE on corrosion of carbon steels (J55, N80, P110SS and C110 steels) in 3.5 wt.% NaCl solution saturated with CO_2 was evaluated using static high pressure and high temperature (HPHT) autoclave. The surface was further evaluated by X-ray diffraction (XRD), scanning electron microscopy (SEM), and contact angle measurements. SEM, XRD, and contact angle measurement studies reveal that the surface of metals are quite unaffected after use of inhibitor in 3.5% NaCl solution saturated with CO_2.

Keywords: *Gingko biloba*; Autoclave; Contact Angle Measurement; SEM; XRD

1. INTRODUCTION

In China, oil and gas field with CO_2 content is mainly distributed in Songliao basin, Bohai gulf basin, Subei-Nanhuanghai basin, Sichuan basin, and Jilin basin. In Songliao region, the CO_2 content of some gas fieid is as high as 99.02%. Gas fields in Bohai gulf basin and Jilin basin also contains high CO_2. Puguang gas field is the highest CO_2 content gas field in Sichuan area, with proportion of 7.94-9.07%. In order to enhance oil recovery in Jilin oil field, liquid CO_2 is injected into the formation

followed by the hot water. Hence the liquid CO_2 and hot water will be miscible to drive the oil out of the formation, which is called miscible displacement to improve oil recovery. However, the CO_2 dissolved in water will lead to severe carbon dioxide corrosion.

Carbon steels are the most commonly used material of construction for petroleum production assets. Carbon steels are susceptible to severe corrosion in process environments containing carbon dioxide [1]. Natural gas is most likely contains carbon dioxide as part from reservoir fluid composition while in other hand CO_2 can be injected for enhanced oil recovery purposes. As such, corrosion control in carbon dioxide containing media is area of concern for oil field industries. Extensive investigation studies had been carried out to understand and control CO_2 corrosion [2]. CO_2 dissolves in oil wells produced water forming carbonic acid that in turn dissociates and decrease the solution pH:

$$CO_{2(g)} + H_2O_{(l)} = H_2CO_{3(aq.)} \quad (1)$$

$$H_2CO_{3(aq.)} = H^+ + HCO_3^- \quad (2)$$

$$HCO_3^- = H^+ + CO_3^{2-} \quad (3)$$

CO_2 and H_2S gases in combination with water are the main cause of corrosion in oil and gas production. In addition, it is normal practice to re-inject production water downhole to maintain the reservoir pressure and stability as well as perform water flooding (using seawater or fresh water sources) to drive oil out of the formation. As field ages, the ratio of watery oil in the produced fluids increases and can reach levels of 95% or higher [3]. This rise in water content implies an increase of the corrosion problems. Internal corrosion caused by the produced fluids is the most costly of the corrosion problems in the oil and gas industry since internal mitigation methods cannot be easily maintained and inspected. Therefore, as a field ages, corrosion control becomes more expensive. Approximately 60% of oilfield failures are related to CO_2 corrosion mainly due to inadequate predictive capability and the poor resistance of carbon and low alloy steels to this type of corrosive attack [4]. CO_2 can produce not only general corrosion but also localized corrosion, which is a much more serious problem.

Several chemical compounds have been tested for corrosion inhibition of metals and alloys; however, the compounds having N, S, and O heteroatoms, incorporated in an aromatic system, have been found to possess excellent anticorrosion potential. Because of increasing ecological awareness and strict environmental regulations, as well as the inevitable drive toward sustainable and environmentally benign processes, attention now has been focused on the development of nontoxic alternatives to inorganic and organic inhibitors applied so far [5-10]. In present study we have used GBE contains n-Hexadecanoic acid, Urea, N,N'-dibutyl-N,N'-dimethyl, biflavones, 3-Amino-4-pyrazolecarbonitrile, Acetic acid, 4-methylphenyl ester, 2-Butyl-3-methylpyrazine and polyprenols as shown in Figure 1. The molecules are rich in heteroatoms (O, N, S) which are present in an effective corrosion inhibitor. Inhibition effect of GBE on the corrosion of carbon steels in 3.5% NaCl solution saturated with CO_2 was studied using high pressure and high temperature autoclave. Meanwhile, the steel surface was examined by contact angle, XRD, and SEM techniques.

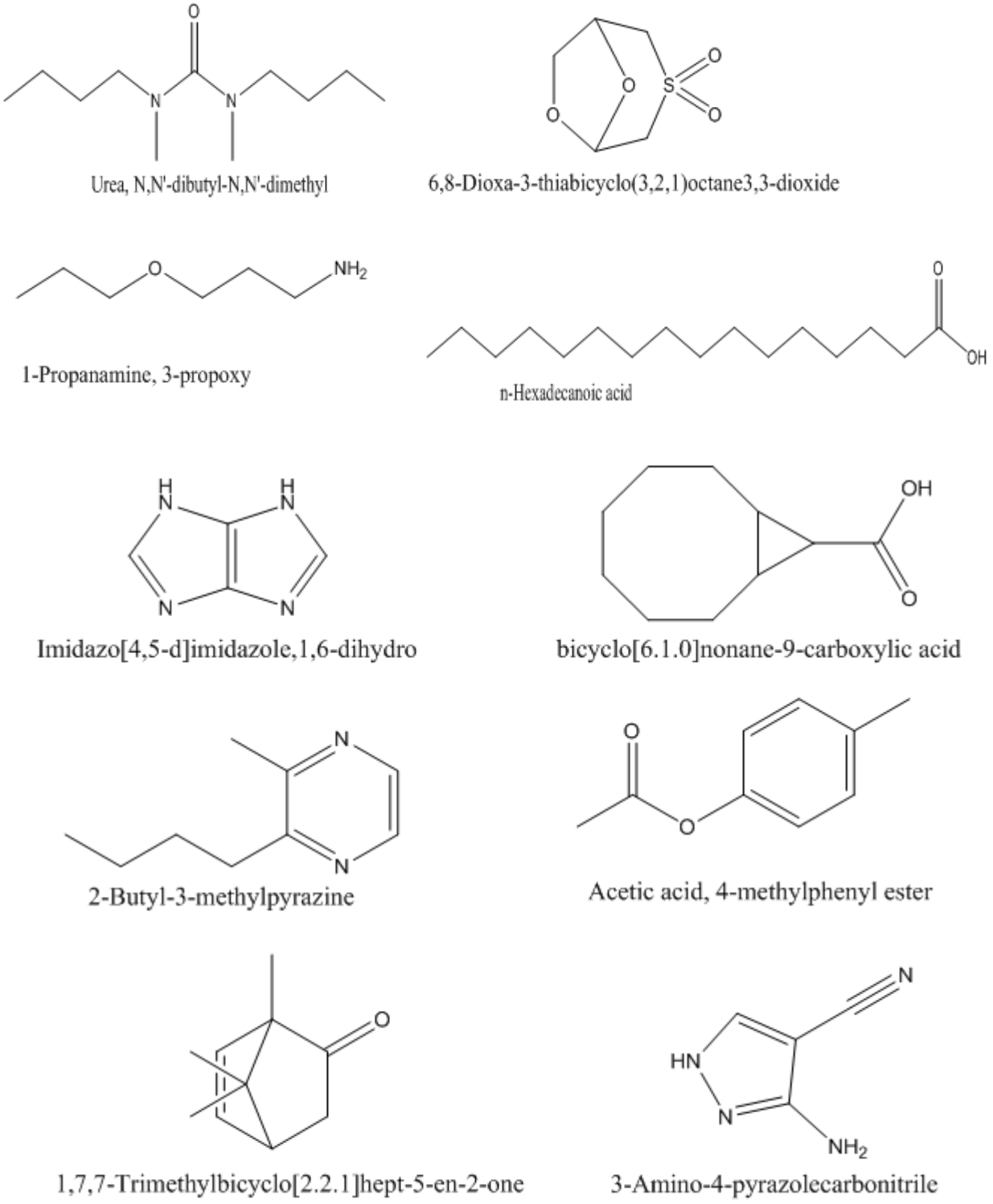

Figure 1. Active constituents present in GBE.

2. EXPERIMENTAL

2.1. Preparation of GBE extract

The leaves of the *Gingko biloba* plant were collected from the field, were dried, and powdered for extraction. Fifty grams of the powder was soaked in 900 ml of reagent grade ethanol for 24 h and

refluxed for 5 h. The ethanolic solution was filtered and concentrated to 500 ml. A green colored powder was obtained after vacuum drying the solution. The powder was then refluxed in 3.5% NaCl to prepare the stock solution. This solution was used to study the corrosion inhibition properties.

2.2. HPHT Autoclave weight loss method

A static high pressure and high temperature (HPHT) autoclave was used for the weight loss experiments. The HPHT tests uses a metal cage spindle tightly packed with the cover containing flat specimens and the 3.5% NaCl solution. 3 liters of 3.5% NaCl solution was saturated with CO_2 at a pressure of 6 MPa, temperature of 120°C and kept for 7 days (168 hours) to observe the corrosion rate. All the carbon steel coupons were metallographically abraded according to ASTM A262, with fine grade emery papers from 600 to 1200 grade to get a mirror finish and weighed before inserting them into the HPHT autoclave. At completion of the test, the apparatus are allowed to cool. After 7 days the specimens were washed with double distilled water, followed by acetone, and dried thoroughly. Specimens were then inspected, and re-weighed. A corrosion rate in calculated for a specific test time and weight loss. The 3.5% NaCl solution was prepared by dilution of analytical grade NaCl with double distilled water. This test has been extensively used in developing corrosion inhibitors for applications where ultra-high shear conditions caused severe corrosion in oil and gas pipelines.

Corrosion tests were performed on a J55 steel of the following percentage composition (wt.%): C 0.24; Si 0.22; Mn 1.1; P 0.103; S 0.004; Cr 0.5; Ni 0.28; Mo 0.021; Cu 0.019; Fe balance. P110SS steel having the following chemical composition (wt %): C 0.27; Si 0.26; Mn 0.6; P 0.009; S 0.003; Cr 0.5; Ni 0.25; Mo 0.6; Nb 0.05; V 0.005; Ti 0.02; Fe balance were used for all studies. N80 steel having the following chemical composition (wt %): C 0.31; Si 0.19; Mn 0.92; P 0.010; S 0.008; Cr 0.2; Fe balance were used for all studies. C110 steel having the following chemical composition (wt %): C 0.35; Mo 0.25; Mn 1.2; Ni 0.99; P 0.02; S 0.005; Cr 1.5; Fe balance were used for all studies.

The inhibition efficiency ($\eta\%$) was determined by using following equation:

$$\eta\% = \frac{w_0 - w_i}{w_0} \times 100 \quad (1)$$

where, w_i and w_0 are the weight loss values in presence and absence of inhibitor, respectively.

The corrosion rate (C_R) of mild steel was calculated using the relation:

$$C_R\,(mm/y) = \frac{87.6 \times w}{atD} \quad (2)$$

where, w is corrosion weight loss of mild steel (mg), a the area of the coupon (cm^2), t is the exposure time (h) and D the density of mild steel ($g\ cm^{-3}$).

2.3. Characterization of GBE

2.3.1. Fourier Transform Infrared Spectroscopy (FTIR)

FTIR was carried out by using Fourier Transform Infrared Spectrometer model NICOLET 6700 connected with OMNIC software. The dried and powdered GBE was mixed with KBr, and grinded in agar-mortar, and then mounted onto a metal case that was used for the study.

2.3.2. Mass Spectrometry (MS)

The mass spectrometry was performed on GC7890-MS5975 gas chromatography mass spectroscopy (Agilent, USA) equipped with a HP-5MS capillary column (30 mm × 0.32 mm × 0.25 μm) and quadruple mass spectrometer. Carrier gas used for the process was, He (1 mL / min). Relative component concentrations were calculated based on peak areas without using correction factors.

2.4. Surface Analyses

2.4.1. UV-Visible spectroscopy

The 3.5% NaCl solution saturated with CO_2 containing 1000 ppm of GBE before and after immersion of carbon steel strips for 168 hours was subjected to UV-Visible absorption detection using UV-5100 double beam spectrophotometer. The solution containing carbon steel strips incubated in the GBE solution (1000 ppm) was taken out followed by thorough dip washing in water. The GBE solution without carbon steels and the washing solution obtained through dip washing of carbon steels were subjected to UV-Visible absorption detection.

2.4.2. X-Ray Diffraction (XRD)

The carbon steel specimens were immersed in 3.5% NaCl solution saturated with CO_2 in absence and presence of inhibitor for a period of 7 days. After then, the specimens were taken out and dried. The film formed on the surface of the steel specimens was analyzed by using X-ray diffractometer, X Pert PRO incorporated with Higscore software.

2.4.3. Contact Angle Measurement

Contact angle measurements were performed using sessile drop technique using DSA100 Kruss optical contact angle measurement instrument made in Germany. Carbon steel samples were carefully cleaned to avoid the surface contaminations, which influence the contact angle measurements through contamination of the liquid when the latter is put in to contact with the sample surface.

2.4.4. Scanning Electron Microscopy (SEM)

The electrodes were immersed in 3.5% NaCl solution saturated with CO_2 in the absence and presence of corrosion inhibitor to observe the effect of corrosion and inhibition. The carbon steel electrodes were then dried at ambient temperature. Micrographs of abraded and corroded carbon steel surfaces and those after inhibitor addition were taken using a SEM model TESCAN VEGA II XMH instrument.

3. RESULTS AND DISCUSSION

3.1 Characterization of GBE

3.1.1. Fourier Transform Infrared Spectroscopy (FTIR)

The peaks obtained as in Figure 2 are 933.10 cm^{-1} -OH group/ olefin's single substitution; 995.84 cm^{-1} C-O bending; 1082.11 cm^{-1} C-O stretching; 1246.81 cm^{-1} C=C (Aromatic)/ C-O stretching; 1399.75 cm^{-1} C=C (Aromatic); 1458.57 cm^{-1} C-H bending; 1513.47 cm^{-1} N-H stretching; 1638.95 cm^{-1} C=C stretching; 2850.67 cm^{-1} –CH stretching vibration; 2925.17 cm^{-1} –CH stretching/ OH group.

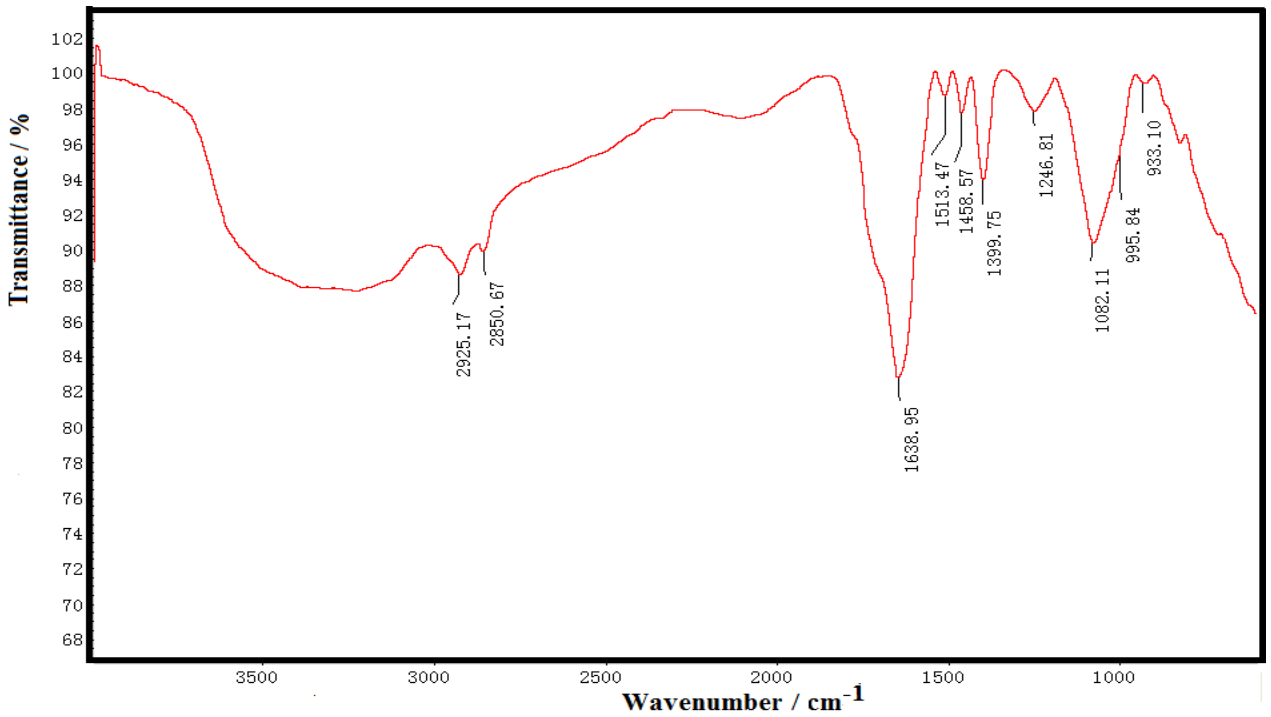

Figure 2. FTIR analysis of GBE.

3.1.2. Mass Spectrometry (MS) Analysis

A number of prominent peaks were identified in the repeated MS analyses of GBE as shown in Figure 3. Among the peaks identified, they are very similar to glycosides, simple phenolic acids, alkylphenols and polyprenols. All the peaks in Figure 3 were matched in NIST (National Institute of Standards and Technology) library with their individual CAS number to get the exact information about the peaks, and the results are #20366: 028564-83-2: 4H-Pyran-4-one, 2,3-dihydro-3,5-dihydroxy-6-methyl, #20367: 028564-83-2: 4H-Pyran-4-one, 2,3-dihydro-3,5-dihydroxy-6-methyl, #20368: 028564-83-2: 4H-Pyran-4-one, 2,3-dihydro-3,5-dihydroxy-6-methyl, 100% at m/z 43.1, 72.0% at m/z 44.1, 46.9% at m/z 144.0, 37.3% at m/z 101.0, 27.1% at m/z 55.1.

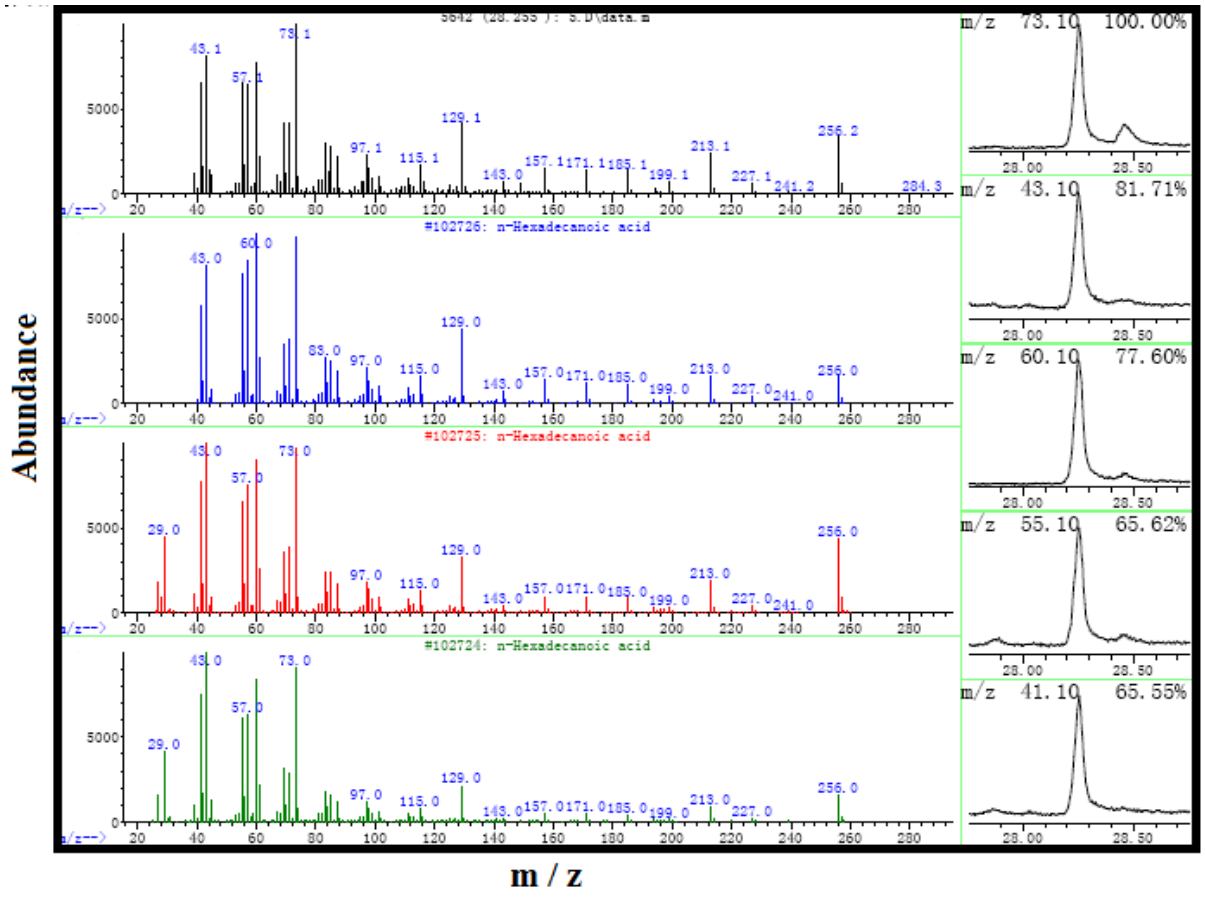

Figure 3. Mass spectrometry for GBE.

3.2. HPHT Autoclave weight loss test

Table 1. Corrosion parameters for different steels in 3.5% NaCl in presence and absence of different concentrations of GBE from weight loss measurements at 120°C after 7 days

Steels	Weight loss	C_R	η
	(mg cm^{-2})	(mm y^{-1})	(%)
C11O with 3.5% NaCl	64	0.341126	-
C11O with inhibitor	28	0.14256	58
P11OSS with 3.5% NaCl	50	0.287932	-
P11OSS with inhibitor	13	0.074862	74
N80 with 3.5% NaCl	49	0.282173	-
N80 with inhibitor	05	0.028793	89
J55 with 3.5% NaCl	51	0.293691	-
J55 with inhibitor	02	0.011517	96

To study the effect of inhibitor concentration (5 mL/L) on the inhibition efficiency, weight loss experiments were carried out in 3.5% NaCl solution saturated with CO_2 at 120°C for 7 days (168 hours) immersion period. The GBE showed inhibition efficiency of 58% for C110 steel, 74% for

P110SS steel, 89% for N80 steel and maximum inhibition efficiency of 96% for J55 steel. Triplicate samples of carbon steel were used to get the accurate values of corrosion rate and inhibition efficiency. The values of percentage inhibition efficiency (η%) and corrosion rate (C_R) obtained from weight loss method of GBE at 120°C are summarized in Table 1.

3.3. Surface Analyses

3.3.1. UV-Visible Spectroscopy Analysis

UV-Visible spectroscopy provides strong evidence for the formation of a metal complex. We obtained UV-Visible absorption spectra for optimum concentration of GBE before and after 168 hours immersion of steel specimens. The electronic absorption spectrum of GBE before the steels immersion shows two bands in UV-region as depicted in Figure 4. These bands may arise due to π-π* and n- π* transitions with a considerable charge transfer character. After 168 hours immersion of steel samples change in the position of absorption maximum or change in the values of absorbance indicate the formation of a complex between two species in solution. However, there was no significant change in the shape of the spectra. These observations provide a strong evidence of complex formation between inhibitor molecules and steel surface and formation of a protective film of inhibitor on the steel surface.

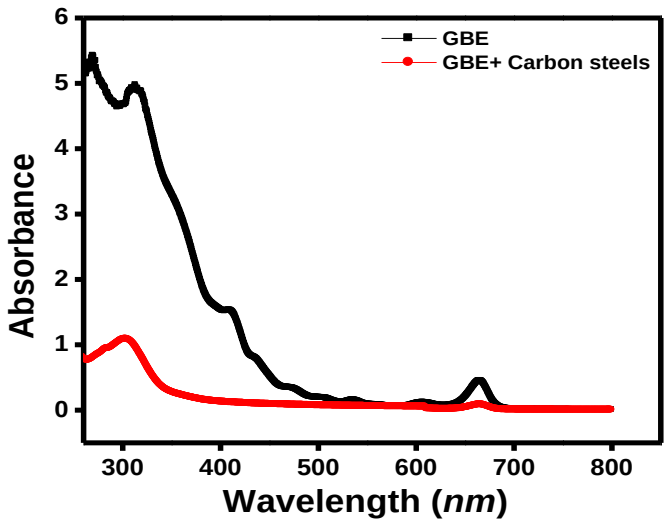

Figure 4. UV-visible spectra for GBE.

3.3.2. X-Ray Diffraction (XRD)

X-ray diffraction was used to determine the corrosion product and film formation on the carbon steel samples in 3.5% NaCl solution saturated with CO_2. The corrosion product over the surface of the carbon steel samples is shown in Figure 5a. Peaks at 2θ = 22°, 26°, 30°, 38°, 43°, 45°, 52°, 63°, and 66° can be assigned to the oxides of iron. Thus, it is observed that in absence of inhibitor, the surface

of the metal contains iron oxides of iron. The XRD patterns of inhibited surface (Figure 5b) showed the presence of some groups present in GBE and iron peaks only, the peaks due to oxides of iron are found to be absent [11-12]. The formation of adsorbed protective film on the surface of metal in the presence of GBE is clearly reflected from these observations.

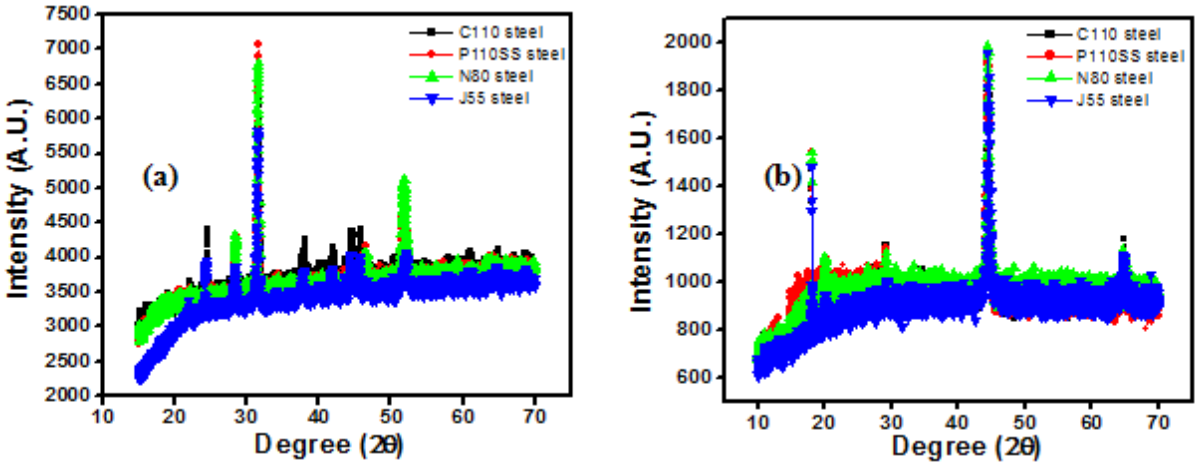

Figure 5. XRD analysis of (a) without GBE and (b) after addition of GBE.

3.3.3. Contact Angle Measurement

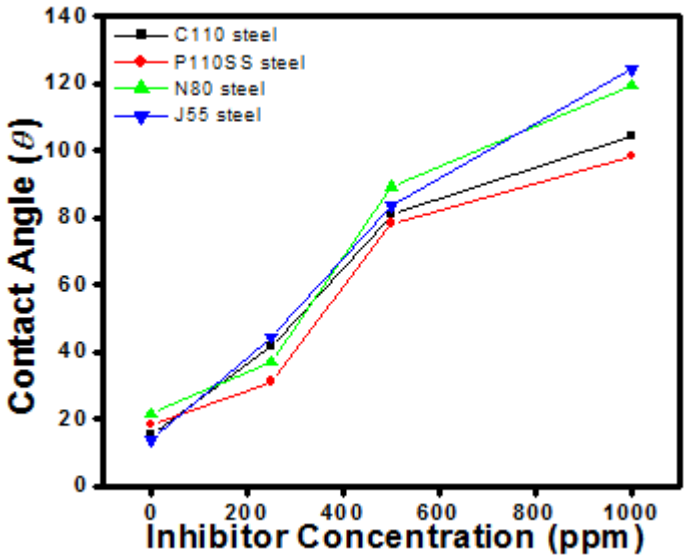

Figure 6. Variation of contact angle with different concentration of GBE on carbon steels surface.

The contact angle measurements were carried out at room temperature. A baseline test without corrosion inhibitor was carried out first after which the corrosion inhibitor package was injected on the carbon steel samples surface and the concentration was increased in steps. Droplets were placed on the

steel surface by 10 microliter syringe. For each concentration of corrosion inhibitor the contact angle measurements were repeated 3 times. The contact angle of carbon steel surfaces without inhibitor was measured as 15.5°, 17.3°, 14.4°, and 16.7° in the 3.5% NaCl solution; meaning that the wettability of steel surface is hydrophilic (favors water). With the addition of inhibitor the contact angle increased for all carbon steel samples and the steel surface became hydrophobic (does not favors water) as is evident from Figure 6. This confirms the formation of a hydrophobic layer on the steel surface in presence of inhibitor.

3.3.4. Scanning Electron Microscopy (SEM)

Scanning electron microscopy photographs were taken to show the corrosion inhibition is due to the formation of an adsorptive film on the carbon steel surface. The morphology of the C110, N80, P110SS, and J55 steel in Figure 7a, 7c, 7e, and 7g showed a corroded surface in the absence of inhibitors.

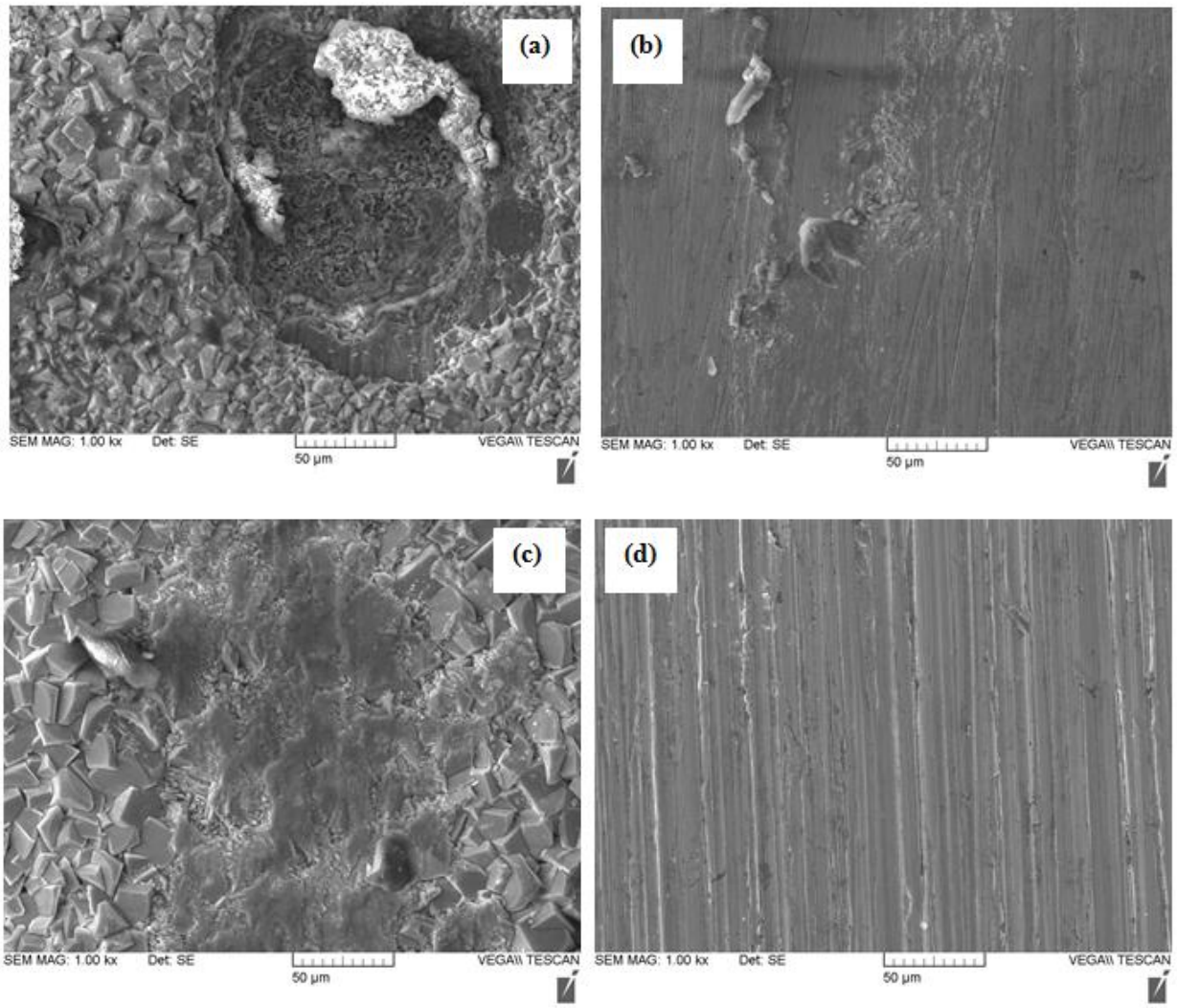

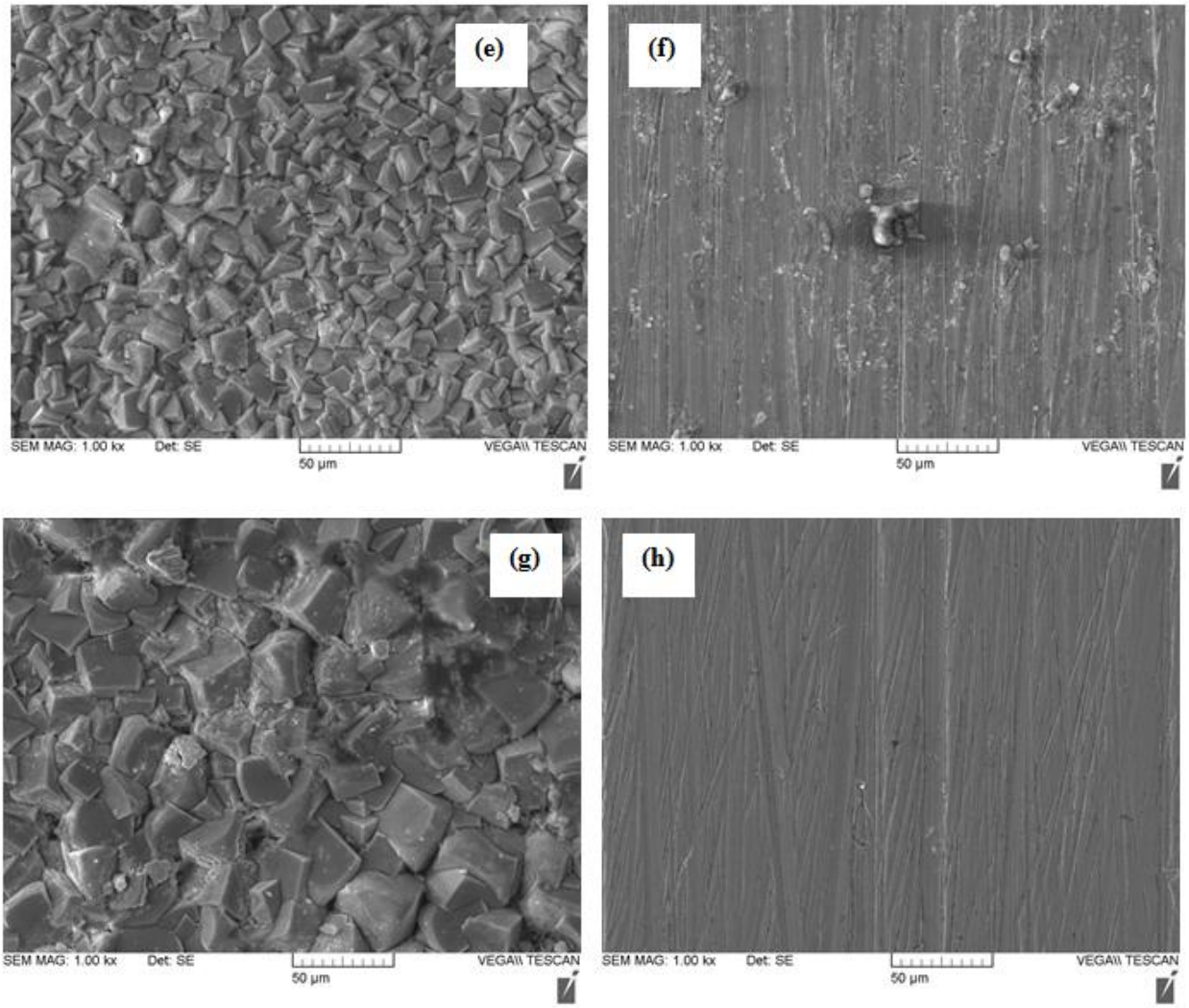

Figure 7. SEM images for (a) 3.5% NaCl solution for C110 steel (b) 1000 ppm GBE C110 steel (c) 3.5% NaCl solution for N80 steel (d) 1000 ppm GBE N80 steel(e) 3.5% NaCl solution for P110SS steel (f) 1000 ppm GBE P110SS steel (g) 3.5% NaCl solution for J55 steel (h) 1000 ppm GBE for J55 steel.

There are pits and cracks on the specimen's surface and the surface is strongly damaged. However, in the presence of GBE, the surface corrosion of steel is remarkably decreased. Figure 7b, 7d, 7f, and 7h showed a perished surface in 3.5% NaCl solution saturated with CO_2 in presence of GBE. Therefore, a smooth and less corroded morphology of steel samples result from exposure to the inhibitor solutions. These results prove that the GBE formed a protective film on the metal surface and can effectively protect steel samples from a corrosive environment.

3.3.5. Mechanism of corrosion mitigation

The inhibition process of steel in the studied environment can be explained by the adsorption of the components of GBE on the metal surface. The adsorption of GBE can be attributed to the presence of N, S and O-atoms and aromatic/heterocyclic rings [13-20]. Therefore, the possible reaction centres

are unshared electron pair of hetero-atoms and π- electrons of aromatic/heterocyclic ring. The adsorption and inhibition effect of GBE in 3.5% NaCl solution saturated with CO_2 can be explained as follows: GBE might be protonated in the solution as follows:

$$\left[\mathrm{GBE} + x\mathrm{H}^{+} \leftrightarrow \mathrm{GBEH}_{\mathrm{x}}\right]^{\mathrm{X}+} \quad (4)$$

Thus, in aqueous solutions, GBE exists either as neutral molecules or in the form of cations (protonated GBE). The neutral GBE may be adsorbed on the metal surface involving the displacement of water molecules from the metal surface. The GBE molecules can be also adsorbed on the metal surface on the basis of donor–acceptor interactions between π-electrons of nitrile group, carbonyl group, and carbon steel samples [21-30]. Also, the GBE molecules may form a hydrophobic film, in contact with the metal surface, thereby retarding corrosion.

4. CONCLUSIONS

1. GBE is a good inhibitor for carbon steels corrosion in 3.5% NaCl solution saturated with CO_2. Inhibition efficiency increases with increasing inhibitor concentration and inhibition efficiency values obtained from different methods employed are in reasonable agreement.
2. Weight loss results from HPHT autoclave showed that J55 steel exhibited highest inhibition efficiency (96%) while C110 steel exhibited lowest inhibition efficiency (58%) among all the carbon steels.
3. The UV-visible, XRD, contact angle, and SEM analyses showed that the inhibition of carbon steels corrosion occurred due to the formation of a protective film on the metal surface through adsorption of the constituents of GBE.

ACKNOWLEDGEMENTS
Authors are thankful for the post doctoral fellowship, financial assistance provided by the National Natural Science Foundation of China (No. 51274170) and the research grants from the Colonel Technology Fund of Southwest Petroleum University (Project No.2012XJZ013).

References

1. B. S. Sanatkumar, J. Nayak, A. N. Shetty, *Int. J. Hydrogen Energ.* 37 (2012) 9431.
2. J. Han, J. William Carey, J. Zhang, *J. Appl. Electrochem.* 41 (2011) 741.
3. W. Bai, J. Yu, Y. Yang, Y. Ye, J. Guo, Y. Zhang, *Int. J. Electrochem. Sci.* 8 (2013) 3441.
4. G. A. Zhang, Y. F. Cheng, *Corros. Sci.* 51 (2009) 87.
5. J. Aljourani, K. Raeissi, M. A. Golozar, *Corros. Sci.* 51 (2009) 1836.
6. R. Solmaz, G. Kardaş, M. Çulha, B. Yazici, M. Erbil, *Electrochim. Acta* 53 (2008) 5941.
7. H. Gerengi, *Ind. Eng. Chem. Res.* 51 (2012) 12835.
8. D. K. Yadav, D. S. Chauhan, I. Ahamad, M. A. Quireshi, *RSC Adv.* 3 (2013) 632.
9. X. Liu, P. C. Okafor, Y. G. Zheng, *Corros. Sci.* 51 (2009) 744.
10. M. Lashgari, A. M. Malek, *Electrochim. Acta* 55 (2010) 5253.

11. A. Singh, Y. Lin, W. Liu, S. Yu, J. Pan, C. Ren, D. Kuanhai, *J. Ind. Eng. Chem.* (2014) http://dx.doi.org/10.1016/j.jiec.2014.01.033.
12. G. Ji, S. K. Shukla, P. Dwivedi, S. Sundaram, R. Prakash, *Ind. Eng. Chem. Res.* 50 (2011) 11954.
13. Y. Abboud, B. Hammouti, A. Abourriche, B. Ihssane, A. Bennamar, M. Charroufi, S. S. Al-Deyab, *Int. J. Electrochem. Sci.* **7 (**2012) 2543.
14. Y. Abboud, B. Hammouti, A. Abourriche, A. Bennamara, H. Hannache, *Res. Chem. Intermed.* 38 (2012) 1591.
15. D. K. Yadav, M. A. Quraishi, *Ind. Eng. Chem. Res.* 51 (2012) 14966.
16. D. K. Yadav, M. A. Quraishi, B. Maiti, *Corros. Sci.* 55 (2011) 254.
17. A. Singh, M.A. Quraishi, E. E. Ebenso, *Int. J. Electrochem. Sci.* 7 (2012) 12545.
18. M. M. Kabanda, I. B. Obot, Eno E. Ebenso, *Int. J. Electrochem. Sci.* 8 (2013) 10839.
19. K.R. Ansari, M.A. Quraishi, Ambrish Singh, *Corros. Sci.* 79 (2014) 5.
20. P. B. Raja, A. K. Qureshi, A. A. Rahim, H. Osman, K. Awang, *Corros. Sci.* 69 (2013) 292.
21. M. A. Quraishi, A. Singh, V. K. Singh, D. K. Yadav, A.K. Singh, *Mater. Chem Phys.* 122(2010) 114.
22. Ambrish Singh, I. Ahamad, V. K. Singh, M. A. Quraishi, *J. Solid State Electr.* 15 (2011) 1087.
23. S. Deng, X. Li, *Corros. Sci.* 55 (2012) 407.
24. Ambrish Singh, I. Ahamad, V. K. Singh, M. A. Quraishi, *Chem. Engg. Comm.* 199 (2012) 63.
25. P.B. Raja, A.A. Rahim, H. Osman, K. Awang, *Int. J. Miner. Metall. Mater.* 18 (2011) 413.
26. A. Lecante, F. Robert, P. A. Blandini, C. Roos, *Curr. Appl. Phys.* 11 (2011) 714.
27. A. Singh, I. Ahamad, M. A. Quraishi, *Arab. J. Chem.* (2013) http://dx.doi.org/ 10.1016/j.arabjc.2012.04.029.
28. A. Singh, Y. Lin, W. Liu, D. Kuanhai, J. Pan, B. Huang, C. Ren, D. Zeng, *J. Taiwan Inst. Chem. Eng.* (2014) http://dx.doi.org/10.1016/j.jtice.2014.02.001.
29. A. Khamis, M. M. Saleh, M.I. Awad, *Corros. Sci.* 66 (2013) 343.
30. A. Singh, M. A. Quraishi, *Res. Chem. Interm.* (2013), http://doi.dx. 10.1007/s11164-013-1398-3.